Title

Detection of nanoparticles in edible plant tissues exposed to nano-copper using single-particle ICP-MS

Journal

Journal of Nanoparticle Research, 20(4)

ISSN

1388-0764

Authors

Keller, Arturo A
Huang, Yuxiong
Nelson, Jenny

Publication Date

2018-04-01

DOI

10.1007/s11051-018-4192-8

Peer reviewed

J Nanopart Res (2018) 20:101
https://doi.org/10.1007/s11051-018-4192-8

RESEARCH PAPER

Detection of nanoparticles in edible plant tissues exposed to nano-copper using single-particle ICP-MS

Arturo A. Keller · Yuxiong Huang · Jenny Nelson

Received: 17 January 2018 / Accepted: 14 March 2018

Abstract The increasing use of nanopesticides has raised concerns about their effects on crop plants and the impact of human health as well as ecological effects. While increased uptake of metal ions has been observed before, to date, very few studies have demonstrated the presence of nanoparticles in edible tissues. Single-particle inductively coupled plasma–mass spectrometry (sp-ICP-MS) has been suggested as a powerful tool to detect inorganic nanoparticles (NPs) in environmental samples. Here, we exposed edible plant tissues from lettuce, kale, and collard green to nano-CuO, simulating its use as a nanopesticide. We applied sp-ICP-MS to demonstrate the presence of nanoparticles, both in the water used to rinse crop leaf surfaces exposed to nano-CuO and within the leaf tissues. Lettuces retained the highest amounts of nCuO NPs on the leaf surface, followed by collard green and then kale. Surface hydrophilicity and roughness of the leaf surfaces played an important role in retaining nano-CuO. The results indicate that most of the nanoparticles are removed via washing, but that a certain fraction is taken up by the leaves and can result in human exposure, albeit at low levels.

Keywords sp-ICP-MS · Copper · Vegetable · Inorganic nanoparticles extraction · Retention · Sensors

This article is part of the topical collection:
20th Anniversary Issue: From the editors

Nicola Pinna, Executive Editor, Mike Roco, Editor-in-Chief

Electronic supplementary material The online version of this article (https://doi.org/10.1007/s11051-018-4192-8) contains supplementary material, which is available to authorized users.

A. A. Keller · Y. Huang
Bren School of Environmental Science and Management, University of California at Santa Barbara, Santa Barbara, CA 93106, USA

A. A. Keller · Y. Huang (✉)
Center for Environmental Implications of Nanotechnology, University of California, Santa Barbara, CA 93106, USA
e-mail: yhuang@bren.ucsb.edu

J. Nelson
Agilent Technologies Inc., Santa Clara, CA, USA

Introduction

Determining the environmental concentrations of engineered nanomaterials (ENMs) is a major challenge for assessing their potential implications. Without this information, it is not possible to establish whether they pose a human or ecological risk. To overcome this challenge, predictive tools (Nowack 2017) have been developed to generate estimates using material flow analysis at global (Keller et al. 2013; Song et al. 2017), continental (Lazareva and Keller 2014; Liu et al. 2014; Sun et al. 2017), regional (Bornhoft et al. 2016; Gottschalk and Nowack 2011; Gottschalk et al. 2013; Keller and Lazareva 2014; Sun et al. 2014), and local levels (Keller and Lazareva 2014; Lazareva and Keller 2014). Detailed fate and transport models have recently been developed to go a step further and predict the residence time of ENMs, their concentrations, and

Published online: 09 April 2018

their accumulation in environmental compartments (e.g., soils, sediments) (Dale et al. 2015; Garner et al. 2017; Liu et al. 2015; Praetorius et al. 2012; Meesters et al. 2014). While these estimates can serve to bridge the gap, they rely on a large number of assumptions and generalizations and have a wide range of uncertainty. Accurate detection of nanoparticles (NPs) in different environmental media is needed, to evaluate the predictions and risk assessments. There are a number of methods available for detecting the presence of inorganic ENMs in different media, with various limitations. In particular, detecting ENMs at the low concentrations predicted (parts per billion or less) to be present in most media is a major challenge. In addition, for ENMs that transform, there are additional challenges in determining whether the NP detected is the original one or a transformed one.

The most common methods for detecting NPs in an aqueous media are dynamic light scattering (DLS) and UV/Vis spectrophotometry. While these approaches have been used extensively to study the behavior of NPs in aqueous media (e.g., aggregation, sedimentation, stability of the suspension) (Adeleye et al. 2014; Burns et al. 1997; Chen and Elimelech 2006; Chowdhury et al. 2012; Conway et al. 2015b; Domingos et al. 2009; Keller et al. 2010; Thio et al. 2011; Tiraferri et al. 2008) and can be used to track NP concentrations over time, they have several limitations. Concentrations have to be sufficiently high (typically > 10 mg/L) for accurate detection; there is no information on NP composition, and in the case of UV/Vis, the wavelength needs to be tailored to the particle in question, bi- or multimodal size fractions cannot be handled well; and the presence of other (e.g., natural or incidental) NPs would seriously affect the measurement. Thus, these approaches cannot be used for more realistic samples (e.g., multimodal size, other non-target NPs). The nanoparticle tracking analysis system (Gallego-Urrea et al. 2011; Mehrabi et al. 2017; Mitrano et al. 2017; Shang and Gao 2014) offers some improvements, since it can track particles with more complex particle-size distributions, but also requires concentrations in the ppm range, provides no information on composition, and would be challenging to use with more realistic samples containing natural and incidental NPs. These approaches will continue to be extremely useful for understanding the fundamental behavior of NPs in different media, but there is a need to be aware of the limitations.

Transmission electron microscopy (TEM) is useful for visually detecting NPs in a sample and may be used to determine the number of particles in a subset of the sample, as well as their shape and size distribution (Hassellöv and Kaegi 2009; Mitrano et al. 2017; Plathe et al. 2013; Shang and Gao 2014; Su et al. 2015; Zhou et al. 2013); a large number of subsamples may be needed to ensure reproducibility. However, the probability of detecting NPs in a sample via TEM decreases rapidly as the NP concentration decreases. Therefore, high to very high initial concentrations are needed for best visualization. Feature composition can be determined using X-ray diffraction and energy-dispersive X-ray spectroscopy (Adeleye et al. 2016; Mitrano et al. 2017; Plathe et al. 2013; Su et al. 2015; Zhou et al. 2013), although confirmation that these indeed are the introduced NPs may be challenging. X-ray absorption near edge structure and extended X-Ray absorption fine structure can also be used to confirm the presence of NPs within a sample, with exquisite precision as to their location within a particular cell or tissue (Gardea-Torresdey et al. 2014; Hernandez-Viezcas et al. 2016; Rui et al. 2015), but also requires high ENM exposure concentrations, as well as access to the beam lines. This method cannot by itself provide information on the concentration of the particles, although it does provide speciation, which can be very useful for confirming the presence of the target ENM.

Single-particle inductively coupled plasma–mass spectrometry (sp-ICP-MS) has the potential for addressing many of these limitations for inorganic NPs. It can provide information on the number of particles in a sample and their mass concentration, particle size, and elemental composition. Laborda et al. present a very detailed explanation of the principles and key considerations for successful sp-ICP-MS (Laborda et al. 2013, 2016). Earlier studies discussed a number of challenges even for the measurement of very well-defined NPs in simple aqueous matrices (Liu et al. 2017; Mitrano et al. 2012, 2014; Reed et al. 2012), but more recent work indicates that this technique is becoming more common for aqueous samples (Montano et al. 2016). As the technique has matured, it has been applied to a wider range of elemental compositions (Frechette-Viens et al. 2017; Lee et al. 2014; Praetorius et al. 2017) and samples (Azodi et al. 2016; Hadioui et al. 2015; Schwertfeger et al. 2016). A few studies have reported the use of sp-ICP-MS in food products, for example to determine the presence of nanoTiO_2 in different

processed foods (Peters et al. 2014) or nanoAg in food stimulants (Linsinger et al. 2014). sp-ICP-MS was also used to track the release of copper-based NPs from an external marine paint (Adeleye et al. 2016). One significant advantage of sp-ICP-MS is the ability to detect NPs at very low concentrations (a few parts per billion) and in fact requires dilution of concentrated samples, overcoming a major limitation in having realistic exposure concentrations.

Copper has been used extensively in agriculture to protect against diseases (Keller et al. 2017), particularly fungal infections and other microbial pathogens (El-Habbaa et al. 2016; Salma et al. 2015). Recently a number of copper-based nanopesticides have been introduced in the market. Early studies indicate that in general, these nanopesticides cause little or no negative physiological effects at the recommended doses, and that in fact, plants may gain biomass when protected with these materials (Elmer and White 2016; Ma et al. 2015; Stampoulis et al. 2009; Trujillo-Reyes et al. 2014; Zuverza-Mena et al. 2015). Metabolomics studies do indicate that several crop plants respond to the exposure to these copper-based nanopesticides by using some of their antioxidants (Zhao et al. 2016a, b, c, d, 2017a, b, c, d, e), as well as upregulating metal chelators and downregulating some organic acids in root exudates (Huang et al. 2017), to minimize the impact of excess copper.

The objective of this study was to detect and quantify the presence of nanoparticles in edible plant tissues exposed to nano-CuO using sp-ICP-MS. Three different types of leaf tissues were evaluated, to determine to what extent leaf surface roughness influences the retention of NPs. In addition, we sought to determine whether NPs would enter the leaf tissues and remain within them even after washing.

Materials and methods

Reagents Ultrapure water (DI) was obtained from a Barnstead NANOpure water purification system (Thermo Scientific, Boston, MA, USA) and used throughout the work. Nitric acid (67–70%) of ultra high purity for quantitative trace metal analysis at the parts-per-trillion (ppt) level (BDH Aristar® Ultra grade) was used to prepare calibration standards. A certified copper reference standard solution of 1000 μg/mL in 2% nitric acid was obtained from High-Purity Standards, Inc. (Charleston, SC, USA).

Nanomaterials Gold NPs with nominal diameters of 60 ± 4 nm were purchased from nanoComposix (San Diego, CA) as bare, dispersible, gold nanospheres in aqueous suspension (2 mM sodium citrate) and are hereafter referenced by their nominal diameters.

Uncoated nano-CuO was purchased from U.S. Research Nanomaterials (Houston, TX, USA); a detailed characterization was presented in a previous study (Adeleye et al. 2014). Briefly, the primary particle size is 20–100 nm (as provided by the manufacturer) and the hydrodynamic diameter (HDD) is 280 ± 15 nm in DI water at pH 7 (0.5 mM phosphate buffer). The surface charge in 0.5 mM phosphate buffer solution is − 34.4 ± 0.5 mV at pH 7, with the isoelectric point (IEP) at 6.3. The helium density of nano-CuO is 6.349 g/cm^3 with 74.3 ± 1.2 wt% copper content and the balance is oxygen.

Leaf tissues Three USDA organic vegetables were purchased on the day of the experiment to ensure freshness. The vegetables, kale (*Brassica oleracea*, var. *Acephala Lacinato*), lettuce (*Lactuca sativa* var. *green leaf cultivar*), and collard green (*Brassica oleracea*, var. *Acephala*) were produced by Cal-Organic Farms (Bakersfield, CA, USA). The surface roughness of the leaf tissues and microscale details were visualized using an environmental scanning electron microscope (ESEM, Philips Electron Optics, Eindoven, The Netherlands).

Exposure and retention of nanoparticles To quantitatively analyze the exposure and retention of nano-Cu onto leaf tissues, vegetable leaves from each type were cut into a 75 × 75 mm square (Fig. S1). Nano-CuO was suspended in DI water and sonicated for 30 min before being applied to the leaf tissues. Ten drops of 20 μL nano-CuO suspension (1 mg/L particle concentration) were evenly spread onto each leaf square with an analytical pipette to ensure that all the vegetable tissues were exposed to equal amounts of nano-CuO (Fig. S2). The final amount of nano-CuO applied onto leaf tissues was 34.4 g/m^2, based on the recommendation for copper-based nanopesticides (Conway et al. 2015a). The sprayed-on nano-CuO suspension was air-dried on the surface of the leaf tissues for 2 h (Fig. S3). Then, the nano-CuO-exposed leaves were rinsed three times with 10 mL DI water, and the drained water of each rinse cycle was collected in metal-free polypropylene tubes (VWR International, West Chester, PA, USA). The collected rinse water samples were analyzed via sp-ICP-

MS to detect NPs and determine the size and particle concentration of nano-CuO. Triplicates from each type of vegetable leaves were treated; control samples were also rinsed following the same procedure. The morphology and particle size of nano-CuO before and after application were studied via electron microscopy using a FEI Tecnai G2 Sphera 200 kV TEM.

Enzymatic digestion To investigate if nano-CuO remained on the rinsed leaf surfaces or entered the leaf tissues via the stomata, Macerozyme R-10 (bioWORLD, Dublin, OH, USA) was used to digest the plant tissues for NP extraction at neutral pH. Macerozyme R-10 is a multi-component (e.g., cellulase, hemicellulase, and pectinase) enzyme mixture, which has been shown to digest plant tissues without changing the NP size (Dan et al. 2015). Circular pieces of leaf tissue (diameter = 6.35 mm) were cut near the area where nano-CuO was applied and also downstream of rinse water runoff, after each rinse (Fig. S3). Each sample was digested in 2 mL of the enzyme solution (containing 100 mg R-10 powder). The samples were shaken with the enzyme solution at 25 °C for 24 h to ensure complete digestion of leaf tissues. A final centrifugation of the digested samples at 20,000×g was done for 20 min, and then the supernatant (0.1 mL) was diluted 100 times for sp-ICP-MS analysis.

sp-ICP-MS measurement An Agilent 7900 ICP-MS (Santa Clara, CA, USA) equipped with standard nickel sampling and skimmer cones, standard glass concentric nebulizer, quartz spray chamber, and small internal diameter (1.0 mm) quartz torch was used to perform sp-ICP-MS analysis to determine the particle size and concentration in all collected samples. Samples were introduced directly into the ICP-MS with the standard peristaltic pump and tubing (i.d. 1.02 mm). Analyses were performed in time-resolved analysis (TRA) mode using an integration time (dwell time) of 100 μs per point with no settling time between measurements. The instrumental settings used for the sp-ICP-MS analysis are summarized in Table 1. The sp-ICP-MS method setup, data collection, and analysis were conducted via the Single Nanoparticle Application Module (method wizard) in the Agilent ICP-MS MassHunter software (Version C.01.03 Build 505.16 Patch 3).

The 60 nm gold NP standard was diluted to 100 ng/L Au (99%) with DI in metal-free polypropylene tubes, to evaluate the nebulization efficiency to be used in the data conversion from raw signal to NP size. A Cu ionic standard of 1 μg/L was prepared with 1% HNO_3 and was used to determine the elemental response factor. The samples were diluted with DI water to ensure the nano-CuO particle concentration was between 10 and 100 ng/L, and a sample inlet flow of 0.346 mL/min was used. Analyte mass fraction was set to 0.75 while CuO particle density was set to 6 g/cm^3. NP sample preparation and dilution were performed on the day of the analysis to avoid sample degradation and minimize nano-CuO dissolution after processing. Before dilution of the samples and again prior to their analysis, all solutions were placed in an ultrasonic bath for 10 min to ensure that the samples were fully homogenized.

Table 1 Optimized instrumental setting for the nano-CuO analysis in sp-ICP-MS (Agilent 7900)

Parameter	Value
RF power	1550 W
Carrier gas	0.67 L/min
Spray chamber temperature	2 °C
Nebulizer pump	0.1 rps
Sample depth	8.0 mm
Integration time	100 μs
Acquisition time	60 s
Mass monitored	^{63}Cu

Results and discussion

Characteristics of nano-CuO Nano-CuO as received forms agglomerates of 30–100 nm-size particles, shown in TEM images (Fig. 1a), which agrees with the size information provided by the manufacturer (20–100 nm). Individual 30–50 nm nano-CuO primary particles can be identified in Fig. 1b. In DI, agglomerates exhibited a larger size of 500–1000 nm (Fig. 1c). The TEM images indicate most of the primary nano-CuO particles are nearly spherical, while the aggregates appeared as rods and flakes (Fig. 1c). NP morphology is important for the accuracy of particle size measurements since NP sizes are calculated based on the assumption that the NPs are spherical (Sannac 2015). Thus, the measured size of nano-CuO agglomerates by sp-ICP-MS may show some difference from other techniques, for example, TEM. In

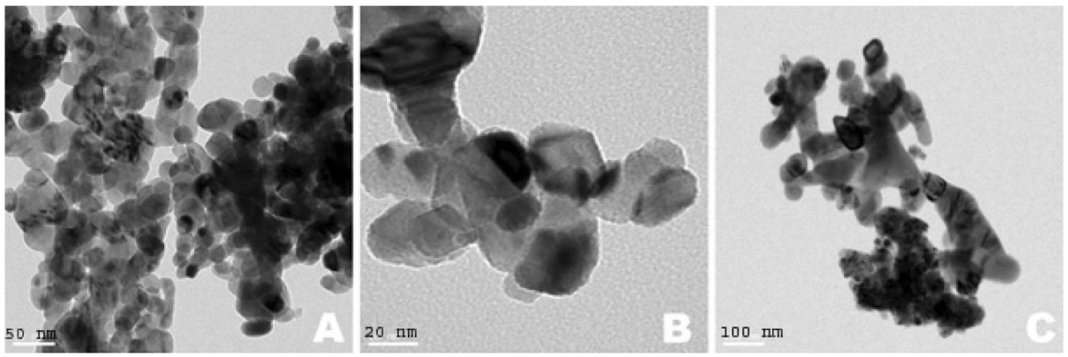

Fig. 1 TEM images of nano-CuO with a scale bar of **a** 50, **b** 20, and **c** 100 nm

a previous study (Adeleye et al. 2014), the same nano-CuO were characterized with dynamic light scattering (Malvern Zetasizer Nano-ZS90) to obtain the HDD, which was reported as 280 ± 15 nm in DI water at pH 7 (0.5 mM phosphate buffer).

The calibration of nano-CuO concentration in DI water was obtained by analyzing from 1 to 500 ng/L (Fig. 2a), with very good linearity ($R^2 = 0.993$) across the entire concentration range. When the nominal nano-CuO concentration was higher than 100 μg/L (e.g., 250 and 500 μg/L), the measured nano-CuO concentration exhibited a larger root square difference (RSD ~ 12%), indicating decreased precision. Similar RSD values were obtained when the nominal nano-CuO concentration was lower than 10 μg/L (e.g., at 1 μg/L, RSD = 9.1%), which suggests the optimal particle concentration for analysis is between 10 and 100 μg/L (RSD < 5%). In the following experiments, all the samples were diluted to the concentration range of 10–100 μg/L as nano-CuO.

Table 2 summarizes the ionic Cu concentration, median size, and mean size of nano-CuO aqueous samples as measured by sp-ICP-MS. The ionic Cu concentration reflects the dissolved fraction within the initial nano-CuO suspension. As the nominal nano-CuO concentration increased, the detected/calculated ionic Cu concentration increased more markedly, especially at higher nano-CuO concentrations (e.g., 250 and 500 μg/L nano-CuO). Since the nano-CuO suspension was prepared fresh on the day of analysis, minimal dissolution of CuO was expected (Adeleye et al. 2014). At NP concentrations higher than 100 μg/L, there may be more than one NP per monitored event, or there

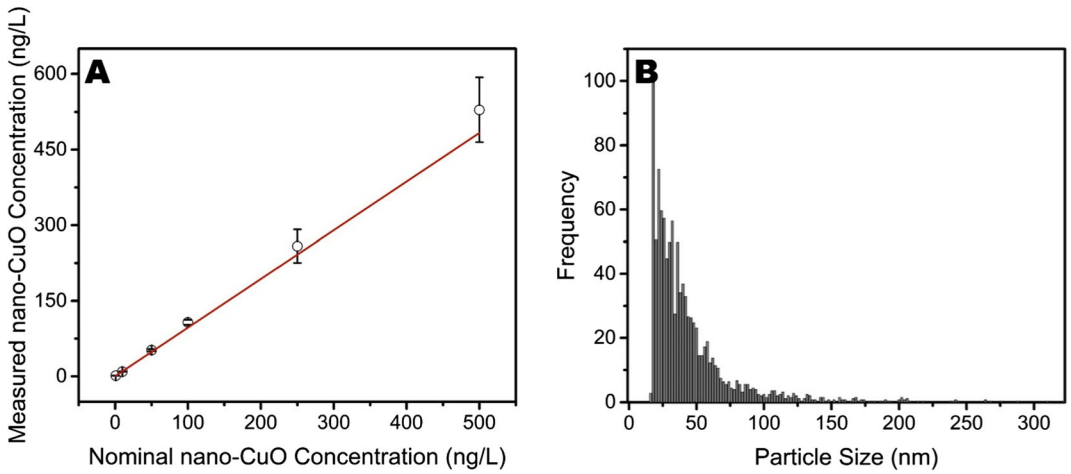

Fig. 2 **a** Calibration curve of nano-CuO concentration in DI water; symbols represent experimental data, and red line represents a linear regression. **b** Size distribution of nano-CuO (at 50 μg/L) measured by sp-ICP-MS.

Table 2 Ionic Cu concentration, median, and mean size of nano-CuO aqueous samples at different nominal nano-CuO concentrations, as measured by sp-ICP-MS

Nominal nano-CuO concentration (ng/L)	Ionic Cu concentration (ng/L)			Median size (nm)			Mean size (nm)		
	Avg.	Std.	RSD (%)	Avg.	Std.	RSD (%)	Avg.	Std.	RSD (%)
1	0.11	0.01	9.3	16.48	0.81	4.9	18.51	1.56	8.4
10	0.39	0.04	10.8	15.99	0.00	0.0	23.62	0.54	2.3
50	2.33	0.06	2.5	24.84	4.40	17.7	36.73	3.62	9.9
100	2.78	0.20	7.3	25.26	2.36	9.3	37.15	2.24	6.0
250	32.12	3.36	10.4	31.76	0.11	0.3	34.01	0.60	1.8
500	35.10	2.47	7.0	31.63	0.10	0.3	34.01	0.72	2.1

could be "carry-over" from the previous event. Thus, at higher NP concentrations, a fraction of the signal may be recorded as dissolved Cu ion instead of CuO NPs, as observed by Montano et al. (2016). Thus, it is best to dilute the nano-CuO samples to < 100 μg/L. The reported median and mean size of nano-CuO ranged from 15 to 37 nm at different nominal nano-CuO concentrations (Table 2). However, the primary particle mean size was in the 24–37 nm range at concentrations > 10 μg/L, with a size distribution from 20 to 210 nm (Fig. 2b), which agrees well with the TEM results. Although the majority of the CuO NPs in solution are agglomerates (Fig. 1), some may be soft agglomerates, releasing primary particles or smaller agglomerates as they pass through the sp-ICP-MS (Fig. 2b).

Characteristics of leaf tissues The surface morphology of selected editable vegetable leaf tissues was characterized via ESEM, as shown in Fig. 3. The lettuce surface had the smoothest texture (Fig. 3a) and was the most hydrophilic with good wettability (Fig. S2A). Kale leaf tissues exhibited the roughest surface with dense texture (Fig. 3c), and very good hydrophobicity with a small contact angle observed when an aqueous droplet was added (Fig. S2C). Collard green also showed good hydrophobicity when interacting with aqueous droplets

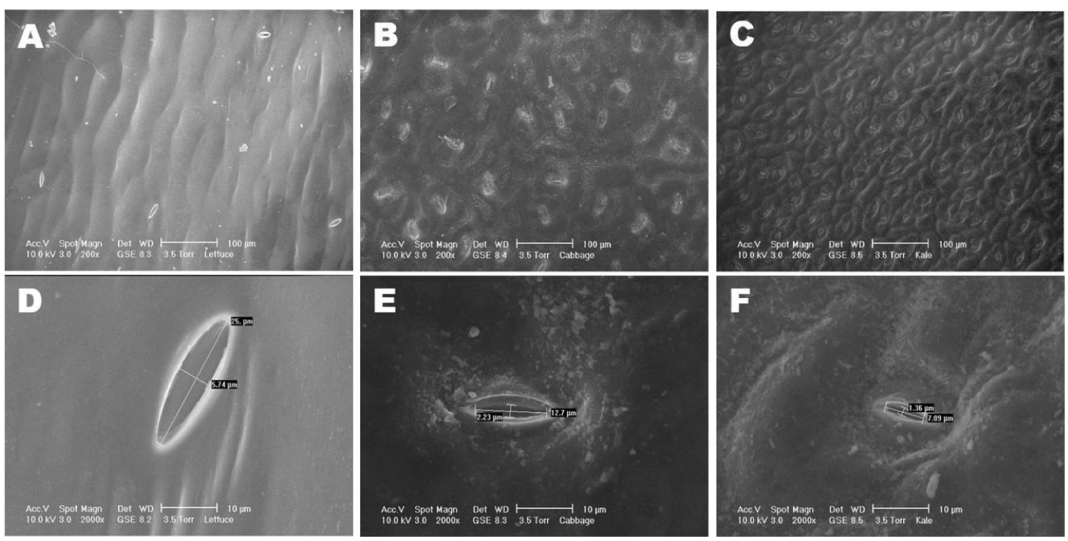

Fig. 3 Surface morphology of **a** green leaf lettuce, **b** collard green, and **c** kale leaf tissues and stomatal openings of **d** green leaf lettuce, **e** collard green, and **f** kale leaf tissues. ESEM images were obtained under a magnification of × 200 and × 2000, respectively

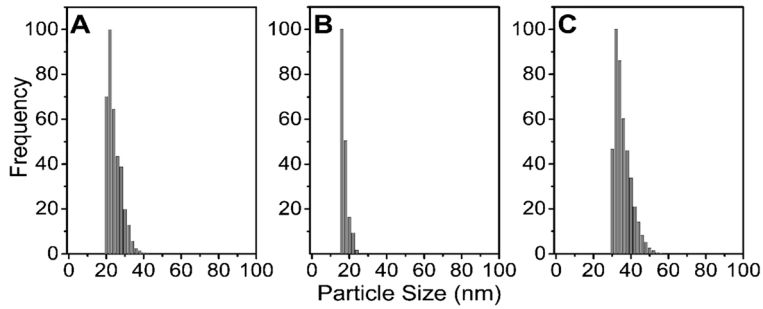

Fig. 4 Particle size distribution of Cu-based nanoparticles from the initial rinse of as-purchased leaf tissues of **a** green leaf lettuce, **b** collard green, and **c** kale. Data obtained via sp-ICP-MS measurement

(Fig. S2B) with some roughness (Fig. 3b). Under higher magnification, the stomatal openings of the various leaves could be observed (Fig. 3d–f). All three species had stomatal openings from 1 to 25 μm; lettuce had the largest stomatal openings while kale had the smallest.

Before applying the nano-CuO suspension onto leaf tissues, 75 × 75 mm samples of as-received leaves were rinsed with 10 mL DI water three times. The collected rinse water was analyzed by sp-ICP-MS to determine whether the unexposed leaves contained nanosized Cu-based particles. As no information was available regarding the shape, density, and composition of these particles, an assumption was made that any initial particles had the same physicochemical properties as nano-CuO (e.g., density, Cu content, and density). In all three leaf types, Cu-based NPs were detected, mostly in the 20–50 nm size range (Fig. 4). However, these NPs were at very low concentration, from 30 to 90 ng/L (Fig. 5) in the first rinse. Additional rinses removed most of these Cu-based NPs. For example, the NP concentrations in the third rinse were 95% less than the first rinse for lettuce and collard green (Fig. 5). The higher roughness of kale (Furmidge 1962) may have shielded some of the NPs from the rinse water, since the third rinse still had 43% of the concentration of the first rinse. These NPs may be from dust in the fields or steps along the distribution chain.

Nano-CuO in leaf tissue rinse water Nano-CuO was detected via sp-ICP-MS in the rinse water of all three leaf tissues after exposure to nano-CuO (Fig. 6). In the first rinse, most of the detected nano-CuO exhibited sizes in the range between 30 and 50 nm (as shown in Fig. 6a, d, g), which agree with the original primary size distribution. Aggregates with particle sizes up to 400 nm were also detected in the first rinse water, although at much lower frequency compared to primary size NPs (Fig. 6a. d. g). In the second rinse cycle, the sizes of nano-CuO particles in the rinse water were larger (Fig. 6b, e, h), especially in the exposed lettuce leaf tissues, with a mean size of 230 nm (Table 3). By the third rinse, the remaining Cu-based NPs have a wide size distribution (Figs. 6c, f, i). These larger NPs may have been trapped in surface crevasses or even stomata and would take more effort to remove via rinsing. The same effect is seen in all three types of vegetables.

Nano-CuO concentrations in the first rinse water were around 500–750 μg/L (Fig. 7, note the logarithmic scale), with the highest concentration detected in collard green leaf rinse water (752.5 μg/L), followed closely by kale, and the lowest concentration in lettuce leaves (508.6 μg/L). There is a strong relationship between first rinse water concentration and leaf surface characteristics. Kale leaf has the highest surface hydrophobicity as well as surface roughness (Fig. 3), which likely channels the applied NP suspension and rinse water through a limited region; lettuce leaves are smoother and much more hydrophilic, spreading the

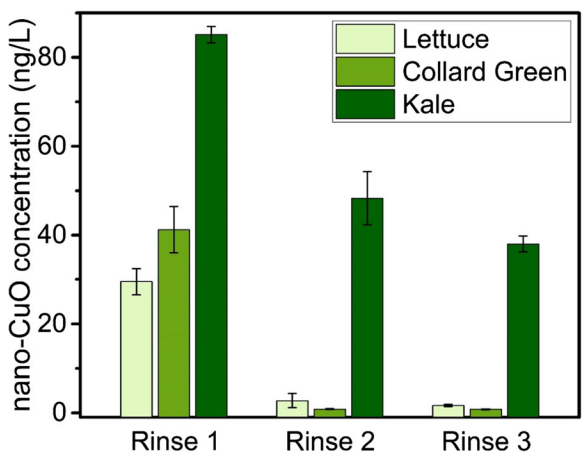

Fig. 5 Cu-based NP concentration in rinse water from as-purchased leaf tissues. Data obtained via sp-ICP-MS measurement

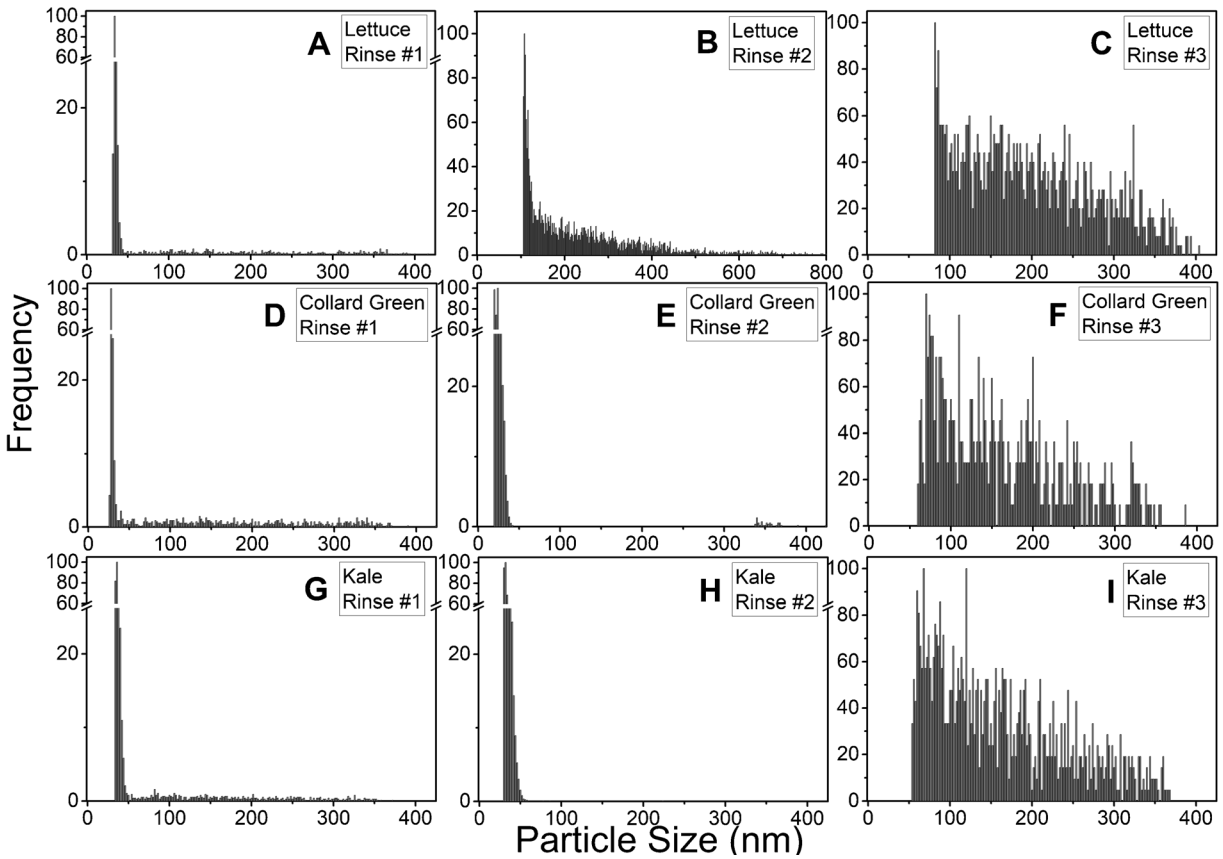

Fig. 6 Particle size distribution in rinse water of nano-CuO exposed lettuce leaves after **a** first rinse, **b** second rinse, and **c** third rinse; collard green leaves after **d** first rinse, **e** second rinse, and **f** third rinse; and kale leaves after **g** first rinse, **h** second rinse, and **i** third rinse. Data obtained via sp-ICP-MS

applied nano-CuO suspension. Thus, nano-CuO were more easily flushed out by the rinse water from the surface of kale and collard green than from lettuce; these results may vary depending on nanopesticide

Table 3 Median and mean size of nano-CuO in rinse water from nano-CuO exposed leaf tissues. Data obtained via sp-ICP-MS

Species	Rinse cycle	Median size (nm)			Mean size (nm)		
		Avg.	Std. Dev.	RSD (%)	Avg.	Std. Dev.	RSD (%)
Lettuce	1	34.80	1.88	5.4	45.61	5.21	11.4
Lettuce	2	233.68	10.51	4.5	187.09	14.46	6.3
Lettuce	3	236.17	12.79	5.4	221.87	17.88	8.1
Collard green	1	30.36	2.53	8.3	78.32	6.09	7.8
Collard green	2	22.92	1.68	7.3	23.76	1.96	8.2
Collard green	3	135.48	13.01	9.6	153.04	11.77	7.7
Kale	1	35.14	2.63	7.5	76.00	3.40	4.5
Kale	2	32.63	0.74	2.3	36.37	3.16	8.7
Kale	3	135.48	13.01	9.6	163.91	11.98	7.3

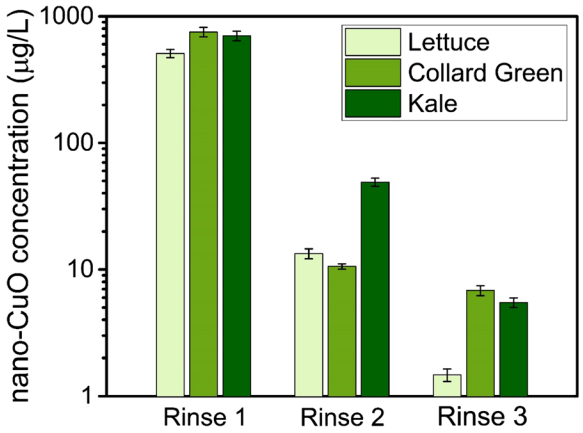

Fig. 7 Particle concentration in rinse water from leaf tissues exposed to nano-CuO. Data obtained via sp-ICP-MS.

application method. The subsequent rinses decreased the nano-CuO concentrations significantly in all three leaf types (Fig. 7), although more pronouncedly in lettuce leaves.

Nano-CuO in leaf tissues Since the stomatal openings of the leaf tissues are in the microscale (Fig. 3), it is possible that nano-CuO enter leaf tissues during the exposure (Zhao et al. 2016b). In addition, some nano-CuO may remain on the leaf surfaces even after several rinses. Figure S4 presents images of the positions where the samples were taken from controls leaves and leaf squares exposed to nano-CuO. Nano-CuO particles were detected in the enzymatically digested leaf tissue samples (Fig. 8). The size distribution of released nano-CuO from the enzymatic digestion ranges from 50 to 150 nm (Fig. 8) and is generally consistent for all three leaf types.

Compared to unexposed controls, nano-CuO concentrations in the exposed crops were 2–3 orders of magnitude greater near the location where nano-CuO was applied (Fig. 9a, note the logarithmic scale). Lettuce retained the highest amount of nano-CuO, followed by collard green and then kale, which was highly related to the stomatal opening sizes on the leaf surfaces (Fig. 3). Lettuce had the largest stomatal openings, making it easier for nano-CuO to enter its tissue (Larue et al. 2014; Zhao et al. 2016b). After the DI water rinse, the residual nano-CuO on or within lettuce tissues decreased significantly from 430 to ~ 180 µg/L, while residual nano-CuO levels on or within collard green (~ 100 µg/L) and kale (~ 45 µg/L) leaf tissues were approximately the same rinse after rinse. This suggests that while lettuce retains the most nano-CuO, it is easiest to remove them via rinsing, in part due to its higher surface hydrophilicity and larger stomatal openings.

For the samples taken further downstream from the position where nano-CuO was applied (see Fig. S4), there were no significant differences in nano-CuO levels between unexposed controls and exposed collard green and kale (Fig. 9b), suggesting that nano-CuO transported by the rinse water is not deposited further downstream for these leaf surfaces. However, nano-CuO concentrations in these downstream locations from exposed lettuce tissues were 10–30-fold higher than control lettuce leaves. The hydrophilic surface on the lettuce leaves may enhance the mobility of nano-CuO.

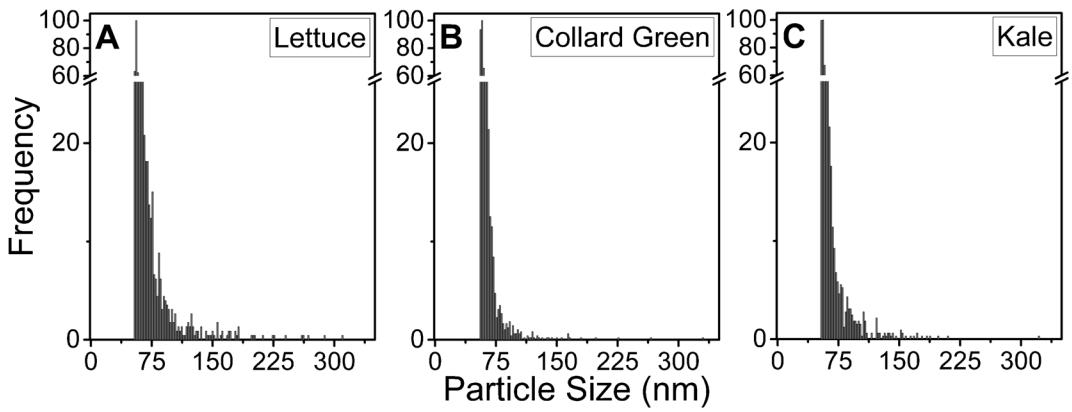

Fig. 8 Nano-CuO particle size distribution in leaves exposed to nano-CuO, rinsed three times and then digested enzymatically: **a** lettuce, **b** collard green, and **c** kale. Data obtained via sp-ICP-MS

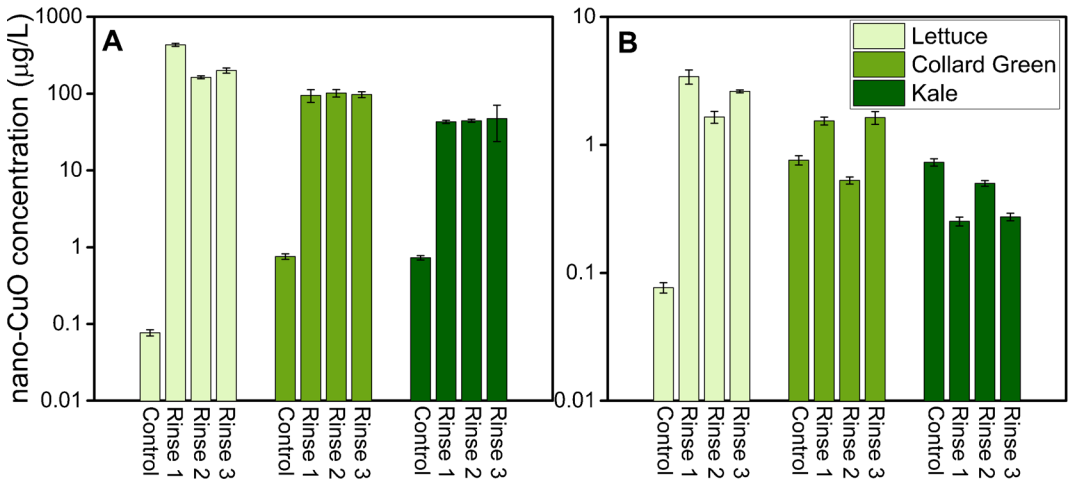

Fig. 9 Particle concentration in enzymatically digested leaf tissues after exposure to nano-CuO spot sampled from positions: **a** close to where the nano-CuO suspension was applied and **b** further downstream of rinse water runoff. Data obtained via sp-ICP-MS.

Thus, nano-CuO may enter lettuce tissues via the stomata during the rinse process as well. Note that the concentrations in these locations are orders of magnitude smaller than near the point of nano-CuO application. In any case, the residual levels of Cu are well below any toxicity concern for humans, based on FDA guidance for daily Cu intake (Zhao et al. 2016a).

Conclusions

We developed a sp-ICP-MS method for detecting NPs in environmental samples, including the water used to rinse exposed crop tissues and plant tissue that were enzymatically digested. sp-ICP-MS can accurately measure nanoparticle size, particle concentration, and dissolved Cu concentration in aqueous samples with low RSD values and very good particle concentration calibration linearity. NPs were detected in the ppb range, and the best conditions for analysis were within 10–100 ppb.

Three different species of edible vegetable leaf tissues, including lettuce, collard green, and kale, were exposed to nano-CuO. Particles were found in all rinse water samples, as individual nanoparticles as well as aggregates. The concentration of nano-CuO in rinse water was highly related to leaf surface characteristics. The highly hydrophilic and smooth lettuce leaves retained fewer nanoparticles after washing. Kale and collard green leaf tissues, with higher surface roughness and somewhat lower hydrophobic affinity, retained more nanoparticles even after three washes. From a practical perspective, washing does remove a significant amount of the nano-CuO, but rougher leaf surfaces will retain more.

Digestion of controls and exposed leaf tissues with macerozyme R-10, followed by sp-ICP-MS analysis, indicates that a substantial fraction of the nano-CuO can remain on the leaf surface or perhaps even enter via the stomata. Lettuce leaves retained the highest amount of nano-CuO within leaf tissues, followed by collard green and then kale. Levels in exposed crops were 2–3 orders of magnitude greater than in unexposed controls. After three cycles of rinse, the residual Cu concentrations were below any toxicity concern for humans (Trumbo et al. 2001).

sp-ICP-MS is a very useful tool which can serve to better understand the interactions between ENMs and plants, including uptake, accumulation, translocation, and biological implications. It can serve to reveal the distribution of nanopesticides in agriculture, whether in runoff water, plant tissues, and wash water. This understanding can be used to design more effective nanopesticides and reduce risk of exposure to humans.

Acknowledgements Any opinions, findings, conclusions, or recommendations expressed in this material are those of the authors do not necessarily reflect the views of the funding agencies.

AAK also appreciates Agilent Technologies for their Agilent Thought Leader Award. The MRL Central Facilities supported by the MRSEC Program of the National Science Foundation under awards NO. DMR 1121053, a member of the NSF-funded Materials Research Facilities Network (www.mrfn.org). We thank the MRL Central Facilities for the use of their TEM instruments and Dr. Aidan Taylor at the UCSB MRL for his help with the TEM measurements.

Funding This study was funded by National Science Foundation (NSF) and the U.S. Environmental Protection Agency (EPA) under NSF-EF0830117.

Compliance with ethical standard

Conflict of interest The authors declare that they have no conflict of interest.

References

Adeleye AS, Conway JR, Perez T, Rutten P, Keller AA (2014) Influence of extracellular polymeric substances on the long-term fate, dissolution, and speciation of copper-based nanoparticles. Environ Sci Technol 48:12561–12568

Adeleye AS, Oranu EA, Tao MY, Keller AA (2016) Release and detection of nanosized copper from a commercial antifouling paint. Water Res 102:374–382. https://doi.org/10.1016/j.watres.2016.06.056

Azodi M, Sultan Y, Ghoshal S (2016) Dissolution behavior of silver nanoparticles and formation of secondary silver nanoparticles in municipal wastewater by single particle ICP-MS. Environ Sci Technol 50:13318–13327. https://doi.org/10.1021/acs.est.6b03957

Bornhoft NA, Sun TY, Hilty LM, Nowack B (2016) A dynamic probabilistic material flow modeling method. Environ Model Softw 76:69–80. https://doi.org/10.1016/j.envsoft.2015.11.012

Burns JL, Yan YD, Jameson GJ, Biggs S (1997) A light scattering study of the fractal aggregation behavior of a model colloidal system. Langmuir 13:6413–6420. https://doi.org/10.1021/la970303f

Chen KL, Elimelech M (2006) Aggregation and deposition kinetics of fullerene (C60) nanoparticles. Langmuir 22:10994–11001

Chowdhury I, Cwiertny DM, Walker SL (2012) Combined factors influencing the aggregation and deposition of nano-TiO2 in the presence of humic acid and Bacteria. Environ Sci Technol 46:6968–6976. https://doi.org/10.1021/es2034747

Conway JR, Beaulieu AL, Beaulieu NL, Mazer SJ, Keller AA (2015a) Environmental stresses increase photosynthetic disruption by metal oxide nanomaterials in a soil-grown plant. ACS Nano 9:11737–11749. https://doi.org/10.1021/acsnano.5b03091

Conway JR, Adeleye AS, Gardea-Torresdey J, Keller AA (2015b) Aggregation, dissolution, and transformation of copper nanoparticles in natural waters. Environ Sci Technol 49:2749–2756. https://doi.org/10.1021/es504918q

Dale AL, Lowry GV, Casman EA (2015) Stream dynamics and chemical transformations control the environmental fate of silver and zinc oxide nanoparticles in a watershed-scale model. Environ Sci Technol 49(12):7285–7293 American Chemical Society. https://doi.org/10.1021/acs.est.5b01205

Dan YB, Zhang WL, Xue RM, Ma XM, Stephan C, Shi HL (2015) Characterization of gold nanoparticle uptake by tomato plants using enzymatic extraction followed by single-particle inductively coupled plasma-mass spectrometry analysis. Environ Sci Technol 49:3007–3014. https://doi.org/10.1021/es506179e

Domingos RF, Tufenkji N, Wilkinson KJ (2009) Aggregation of titanium dioxide nanoparticles: role of a fulvic acid. Environ Sci Technol 43:1282–1286. https://doi.org/10.1021/es8023594

El-Habbaa G, Abdou M, El-Shaery S (2016) Biological and chemical control of grapevine die-back disease and their effect on defense related enzymes. Int J Sci Eng Res 7:345–351

Elmer WH, White JC (2016) The use of metallic oxide nanoparticles to enhance growth of tomatoes and eggplants in disease infested soil or soilless medium. Environ Sci: Nano 3:1072–1079

Frechette-Viens L, Hadioui M, Wilkinson KJ (2017) Practical limitations of single particle ICP-MS in the determination of nanoparticle size distributions and dissolution: case of rare earth oxides. Talanta 163:121–126. https://doi.org/10.1016/j.talanta.2016.10.093

Furmidge C (1962) Physico-chemical studies on agricultural sprays. IV.—the retention of spray liquids on leaf surfaces. J Sci Food Agric 13:127–140

Gallego-Urrea JA, Tuoriniemi J, Hassellov M (2011) Applications of particle-tracking analysis to the determination of size distributions and concentrations of nanoparticles in environmental, biological and food samples. Trac-Trend Anal Chem 30:473–483. https://doi.org/10.1016/j.trac.2011.01.005

Gardea-Torresdey JL, Rico CM, White JC (2014) Trophic transfer, transformation, and impact of engineered nanomaterials in terrestrial environments. Environ Sci Technol 48:2526–2540. https://doi.org/10.1021/es4050665

Garner KL, Suh S, Keller AA (2017) Assessing the risk of engineered nanomaterials in the environment: development and application of the nanoFate model. Environ Sci Technol 51(10):5541–5551. https://doi.org/10.1021/acs.est.6b05279

Gottschalk F, Nowack B (2011) The release of engineered nanomaterials to the environment. J Environ Monit 13:1145–1155. https://doi.org/10.1039/c0em00547a

Gottschalk F, Sun TY, Nowack B (2013) Environmental concentrations of engineered nanomaterials: review of modeling and analytical studies. Environ Pollut 181:287–300. https://doi.org/10.1016/j.envpol.2013.06.003

Hadioui M, Merdzan V, Wilkinson KJ (2015) Detection and characterization of ZnO nanoparticles in surface and waste waters using single particle ICPMS. Environ Sci Technol 49:6141–6148. https://doi.org/10.1021/acs.est.5b00681

Hassellöv M, Kaegi R (2009) Analysis and Characterization of Manufactured Nanoparticles in Aquatic Environments. In: Analysis and characterization of manufactured nanoparticles in aquatic environments. Wiley, Hoboken

Hernandez-Viezcas JA, Castillo-Michel H, Peralta-Videa JR, Gardea-Torresdey JL (2016) Interactions between CeO2 nanoparticles and the desert plant mesquite: a spectroscopy approach. ACS Sustain Chem Eng 4:1187–1192

Huang YX, Zhao LJ, Keller AA (2017) Interactions, transformations, and bioavailability of Nano-copper exposed to root

exudates. Environ Sci Technol 51:9774–9783. https://doi.org/10.1021/acs.est.7b02523

Keller AA, Lazareva A (2014) Predicted releases of engineered nanomaterials: from global to regional to local. Environ Sci Technol Lett 1:65–70. https://doi.org/10.1021/ez400106t

Keller AA, Wang H, Zhou D, Lenihan HS, Cherr G, Cardinale BJ, Miller R, Ji Z (2010) Stability and aggregation of metal oxide nanoparticles in natural aqueous matrices. Environ Sci Technol 44:1962–1967. https://doi.org/10.1021/es902987d

Keller AA, McFerran S, Lazareva A, Suh S (2013) Global life cycle releases of engineered nanomaterials. J Nanopart Res 15:1692

Keller AA, Adeleye AS, Conway JR, Garner KL, Zhao L, Cherr GN, Hong J, Gardea-Torresdey JL, Godwin HA, Hanna S, Ji Z, Kaweeteerawat C, Lin S, Lenihan HS, Miller RJ, Nel AE, Peralta-Videa JR, Walker SL, Taylor AA, Torres-Duarte C, Zink JI, Zuverza-Mena N (2017) Comparative environmental fate and toxicity of copper nanomaterials. Nano 7:28–40. https://doi.org/10.1016/j.impact.2017.05.003

Laborda F, Jimenez-Lamana J, Bolea E, Castillo JR (2013) Critical considerations for the determination of nanoparticle number concentrations, size and number size distributions by single particle ICP-MS. J Anal Atom Spectrom 28:1220–1232. https://doi.org/10.1039/c3ja50100k

Laborda F, Bolea E, Jiménez-Lamana J (2016) Single particle inductively coupled plasma mass spectrometry for the analysis of inorganic engineered nanoparticles in environmental samples. Trends Environ Anal Chem 9:15–23

Larue C, Castillo-Michel H, Sobanska S, Trcera N, Sorieul S, Cécillon L, Ouerdane L, Legros S, Sarret G (2014) Fate of pristine TiO2 nanoparticles and aged paint-containing TiO2 nanoparticles in lettuce crop after foliar exposure. J Hazard Mater 273:17–26. https://doi.org/10.1016/j.jhazmat.2014.03.014

Lazareva A, Keller AA (2014) Estimating potential life cycle releases of engineered nanomaterials from wastewater treatment plants. ACS Sustain Chem Eng 2:1656–1665. https://doi.org/10.1021/sc500121w

Lee S, Bi XY, Reed RB, Ranville JF, Herckes P, Westerhoff P (2014) Nanoparticle size detection limits by single particle ICP-MS for 40 elements. Environ Sci Technol 48:10291–10300. https://doi.org/10.1021/es502422v

Linsinger TPJ, Peters R, Weigel S (2014) International interlaboratory study for sizing and quantification of ag nanoparticles in food simulants by single-particle ICPMS. Anal Bioanal Chem 406:3835–3843. https://doi.org/10.1007/s00216-013-7559-9

Liu HH, Bilal M, Cohen Y, Lazareva A, Keller A (2014) Regional multimedia distribution of nanomaterials and associated exposures: a software platform. In Bioinformatics and Biomedicine (BIBM), 2014 IEEE International Conference on p 10–17

Liu HH, Bilal M, Lazareva A, Keller AA, Cohen Y (2015) Simulation tool for assessing the release and environmental distribution of nanomaterials. Beilstein J Nanotechnol 6(1):938–951 Beilstein-Institut. https://doi.org/10.3762/bjnano.6.97

Liu JY, Murphy KE, Winchester MR, Hackley VA (2017) Overcoming challenges in single particle inductively coupled plasma mass spectrometry measurement of silver nanoparticles. Anal Bioanal Chem 409:6027–6039. https://doi.org/10.1007/s00216-017-0530-4

Ma CX, White JC, Dhankher OP, Xing BS (2015) Metal-based nanotoxicity and detoxification pathways in higher plants. Environ Sci Technol 49:7109–7122. https://doi.org/10.1021/acs.est.5b00685

Meesters JAJ, Koelmans AA, Quik JTK, Hendriks AJ, van de Meent D (2014) Multimedia modeling of engineered nanoparticles with simplebox4nano: model definition and evaluation. Environ Sci Technol 48(10):5726–5736. American Chemical Society. https://doi.org/10.1021/es500548h

Mehrabi K, Nowack B, Dasilya YAR, Mitrano DM (2017) Improvements in nanoparticle tracking analysis to measure particle aggregation and mass distribution: a case study on engineered nanomaterial stability in incineration landfill leachates. Environ Sci Technol 51:5611–5621. https://doi.org/10.1021/acs.est.7b00597

Mitrano DM, Barber A, Bednar A, Westerhoff P, Higgins CP, Ranville JF (2012) Silver nanoparticle characterization using single particle ICP-MS (SP-ICP-MS) and asymmetrical flow field flow fractionation ICP-MS (AF4-ICP-MS). J Anal Atom Spectrom 27:1131–1142. https://doi.org/10.1039/c2ja30021d

Mitrano DM, Ranville JF, Bednar A, Kazor K, Hering AS, Higgins CP (2014) Tracking dissolution of silver nanoparticles at environmentally relevant concentrations in laboratory, natural, and processed waters using single particle ICP-MS (spICP-MS). Environ Sci-Nano 1:248–259. https://doi.org/10.1039/c3en00108c

Mitrano DM, Mehrabi K, Dasilva YAR, Nowack B (2017) Mobility of metallic (nano)particles in leachates from landfills containing waste incineration residues. Environ Sci-Nano 4:480–492. https://doi.org/10.1039/c6en00565a

Montano MD, Olesik JW, Barber AG, Challis K, Ranville JF (2016) Single particle ICP-MS: advances toward routine analysis of nanomaterials. Anal Bioanal Chem 408:5053–5074. https://doi.org/10.1007/s00216-016-9676-8

Nowack B (2017) Evaluation of environmental exposure models for engineered nanomaterials in a regulatory context. Nano 8:38–47. https://doi.org/10.1016/j.impact.2017.06.005

Peters RJB, van Bemmel G, Herrera-Rivera Z, Helsper HPFG, Marvin HJP, Weigel S, Tromp PC, Oomen AG, Rietveld AG, Bouwmeester H (2014) Characterization of titanium dioxide nanoparticles in food products: analytical methods to define nanoparticles. J Agric Food Chem 62:6285–6293. https://doi.org/10.1021/jf5011885

Plathe KL, von der Kammer F, Hassellov M, Moore JN, Murayama M, Hofmann T, Hochella MF (2013) The role of nanominerals and mineral nanoparticles in the transport of toxic trace metals: field-flow fractionation and analytical TEM analyses after nanoparticle isolation and density separation. Geochim Cosmochim Acta 102:213–225. https://doi.org/10.1016/j.gca.2012.10.029

Praetorius A, Scheringer M, Hungerbuhler K (2012) Development of environmental fate models for engineered nanoparticles—a case study of TiO2 nanoparticles in the Rhine River. Environ Sci Technol 46(12):6705–6713. https://doi.org/10.1021/es204530n

Praetorius A, Gundlach-Graham A, Goldberg E, Fabienke W, Navratilova J, Gondikas A, Kaegi R, Günther D, Hofmann T, von der Kammer F (2017) Single-particle multi-element fingerprinting (spMEF) using inductively-coupled plasma time-of-flight mass spectrometry (ICP-TOFMS) to identify engineered nanoparticles against the elevated natural

background in soils. Environ Sci-Nano 4:307–314. https://doi.org/10.1039/c6en00455e

Reed RB, Higgins CP, Westerhoff P, Tadjiki S, Ranville JF (2012) Overcoming challenges in analysis of polydisperse metal-containing nanoparticles by single particle inductively coupled plasma mass spectrometry. J Anal Atom Spectrom 27:1093–1100. https://doi.org/10.1039/c2ja30061c

Rui YK, Zhang P, Zhang Y, Ma Y, He X, Gui X, Li Y, Zhang J, Zheng L, Chu S, Guo Z, Chai Z, Zhao Y, Zhang Z (2015) Transformation of ceria nanoparticles in cucumber plants is influenced by phosphate. Environ Pollut 198:8–14. https://doi.org/10.1016/j.envpol.2014.12.017

Salma B, Devi N, Marak T, Nath P, Saha J (2015) In vitro efficacy of some commercial fungicides against Colletotrichum capsici, the causal agent of anthracnose of chilli. Environ Ecol 33:1863–1866

Sannac S (2015) Single particle analysis of nanomaterials using the Agilent 7900 ICP-MS An Agilent Application Note

Schwertfeger DM, Velicogna JR, Jesmer AH, Scroggins RP, Princz JI (2016) Single particle-inductively coupled plasma mass spectroscopy analysis of metallic nanoparticles in environmental samples with large dissolved analyte fractions. Anal Chem 88:9908–9914. https://doi.org/10.1021/acs.analchem.6b02716

Shang J, Gao XH (2014) Nanoparticle counting: towards accurate determination of the molar concentration. Chem Soc Rev 43:7267–7278. https://doi.org/10.1039/c4cs00128a

Song RS, Qin YW, Suh S, Keller AA (2017) Dynamic model for the stocks and release flows of engineered nanomaterials. Environ Sci Technol 51:12424–12433. https://doi.org/10.1021/acs.est.7b01907

Stampoulis D, Sinha SK, White JC (2009) Assay-dependent phytotoxicity of nanoparticles to plants. Environ Sci Technol 43:9473–9479. https://doi.org/10.1021/es901695c

Su YM, Adeleye AS, Keller AA, Huang YX, Dai CM, Zhou XF, Zhang YL (2015) Magnetic sulfide-modified nanoscale zerovalent iron (S-nZVI) for dissolved metal ion removal. Water Res 74:47–57. https://doi.org/10.1016/j.watres.2015.02.004

Sun TY, Gottschalk F, Hungerbuhler K, Nowack B (2014) Comprehensive probabilistic modelling of environmental emissions of engineered nanomaterials. Environ Pollut 185:69–76. https://doi.org/10.1016/j.envpol.2013.10.004

Sun TY, Mitrano DM, Bornhoft NA, Scheringer M, Hungerbuhler K, Nowack B (2017) Envisioning Nano release dynamics in a changing world: using dynamic probabilistic modeling to assess future environmental emissions of engineered nanomaterials. Environ Sci Technol 51:2854–2863. https://doi.org/10.1021/acs.est.6b05702

Thio BJR, Zhou DX, Keller AA (2011) Influence of natural organic matter on the aggregation and deposition of titanium dioxide nanoparticles. J Hazard Mater 189:556–563. https://doi.org/10.1016/j.jhazmat.2011.02.072

Tiraferri A, Chen KL, Sethi R, Elimelech M (2008) Reduced aggregation and sedimentation of zero-valent iron nanoparticles in the presence of guar gum. J Colloid Interface Sci 324:71–79. https://doi.org/10.1016/j.jcis.2008.04.064

Trujillo-Reyes J, Majumdar S, Botez C, Peralta-Videa J, Gardea-Torresdey J (2014) Exposure studies of core–shell Fe/Fe 3 O 4 and cu/CuO NPs to lettuce (Lactuca sativa) plants: are they a potential physiological and nutritional hazard? J Hazard Mater 267:255–263

Trumbo P, Yates AA, Schlicker S, Poos M (2001) Dietary reference intakes: vitamin a, vitamin K, arsenic, boron, chromium, copper, iodine, Iron, manganese, molybdenum, nickel, silicon, vanadium, and zinc. J Am Diet Assoc 101(3):294–301. https://doi.org/10.1016/S0002-8223(01)00078-5.

Zhao L, Huang Y, Hannah-Bick C, Fulton AN, Keller AA (2016a) Application of metabolomics to assess the impact of Cu(OH)2 nanopesticide on the nutritional value of lettuce (*Lactuca sativa*): enhanced Cu intake and reduced antioxidants. Nanoimpact 3–4:58–66. https://doi.org/10.1016/j.impact.2016.08.005

Zhao L, Ortiz C, Adeleye AS, Hu Q, Zhou H, Huang Y, Keller AA (2016b) Metabolomics to detect response of lettuce (Lactuca sativa) to cu(OH)2 Nano-pesticides: oxidative stress response and detoxification mechanisms. Environ Sci Technol 50:9697–9707. https://doi.org/10.1021/acs.est.6b02763

Zhao L, Huang Y, Zhou H, Adeleye AS, Wang H, Ortiz C, Mazer SJ, Keller AA (2016c) GC-TOF-MS based metabolomics and ICP-MS based metallomics of cucumber (Cucumis sativus) fruits reveal alteration of metabolites profile and biological pathway disruption induced by nano copper. Environ Sci: Nano 3:1114–1123. https://doi.org/10.1039/C6EN00093B

Zhao L, Huang Y, Hu J, Zhou H, Adeleye AS, Keller AA (2016d) 1H NMR and GC-MS based metabolomics reveal defense and detoxification mechanism of cucumber plant under nano-Cu stress. Environ Sci Technol 50:2000–2010. https://doi.org/10.1021/acs.est.5b05011

Zhao L, Hu Q, Huang Y, Fulton A, Hannah-Bick C, Adeleye A, Keller AA (2017a) Activation of antioxidant and detoxification gene expression in cucumber plants exposed to a cu(OH)2 nanopesticide. Environ Sci: Nano 4:1750–1760. https://doi.org/10.1039/C7EN00358G

Zhao L, Hu J, Huang Y, Wang H, Adeleye A, Ortiz C, Keller AA (2017b) 1H NMR and GC–MS based metabolomics reveal nano-Cu altered cucumber (*Cucumis sativus*) fruit nutritional supply. Plant Physiol Biochem 110:138–146. https://doi.org/10.1016/j.plaphy.2016.02.010

Zhao L, Huang Y, Adeleye AS, Keller AA (2017c) Metabolomics reveals cu(OH)2 Nanopesticide activated antioxidative pathways and decreased beneficial antioxidants in spinach leaves. Environ Sci Technol 51:10184–10194. https://doi.org/10.1021/acs.est.7b02163

Zhao L, Hu Q, Huang Y, Keller AA (2017d) Response at genetic, metabolic, and physiological levels of maize (Zea mays) exposed to a cu(OH)2 Nanopesticide. ACS Sustain Chem Eng 5:8294–8301. https://doi.org/10.1021/acssuschemeng.7b01968

Zhao L, Huang Y, Keller AA (2017e) Comparative metabolic response between cucumber (*Cucumis sativus*) and corn (*Zea mays*) to a Cu(OH)2 nanopesticide. J Agr Food Chem. https://doi.org/10.1021/acs.jafc.7b01306

Zhou DX, Ji ZX, Jiang XM, Dunphy DR, Brinker J, Keller AA (2013) Influence of material properties on TiO2 nanoparticle agglomeration. Plos One 8. https://doi.org/10.1371/journal.pone.0081239

Zuverza-Mena N, Medina-Velo IA, Barrios AC, Tan WJ, Peralta-Videa JR, Gardea-Torresdey JL (2015) Copper nanoparticles/compounds impact agronomic and physiological parameters in cilantro (Coriandrum sativum). Environ Sci-Proc Imp 17:1783–1793. https://doi.org/10.1039/c5em00329f